Thermochimica Acta, 146 (1989) 1–13
Elsevier Science Publishers B.V., Amsterdam – Printed in The Netherlands

THE USE OF THERMAL AND SPECTROMETRIC ANALYSES FOR THE STRUCTURE INVESTIGATION OF ARYLHYDRAZONEACETOACETYLAMINOPYRIDINES AND THEIR COPPER CHELATES

M.A. ZAYED, F.A. NOUR EL-DIEN and M.A.F. SHARAF

Chemistry Department, Faculty of Science, University of Cairo, Giza (Egypt)

(Received 22 December 1987; in final form 28 June 1988)

ABSTRACT

A series of α-arylhydrazoneacetoacetylaminopyridine ligands and their copper(II) complexes have been isolated and characterized. Characterization involves elemental and thermal analyses together with UV, visible, proton magnetic resonance and IR spectral studies. Based on these physicochemical studies, the structural formulae for the obtained ligands and their complexes have been suggested. The suggested formulae of these complexes are CuL·X (L = ligands, X = H_2O or acetate group). Thermal analysis of the ligands and of their isolated complexes have already indicated hydrogen bonding within the ligand molecule and different modes of interaction between the ligands and the central copper(II) metal ions. UV, visible, IR and ^1H NMR spectral studies have also been used to investigate the nature of the hydrogen bonding within the ligands and have indicated that their coordination to the central metal ion is via oxygen- and nitrogen-containing groups. This work is relevant to the applications of these dyes and their complexes in different fields of industry.

INTRODUCTION

Studies of copper(II) complexes have attracted, and will continue to attract, the attention of scientists in a wide field of chemistry; in particular, much interest has been directed towards the synthesis, spectral studies and stability of copper chelates with different ligands [1–7].

Cupric complexes usually assume the square planar form [8] and under favourable conditions tend towards octahedral structures. In addition to these square merging into tetragonally distorted octahedral complexes, there are some stereoforms [9–11].

The present work aims to investigate the structure of the possible copper(II) chelates formed during interaction with α-arylhydrazoacetoacetylaminopyridines L_i ($i = 1–5$).

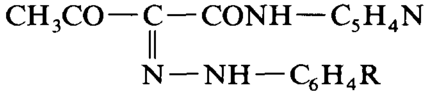

$$\begin{array}{lll} CH_3CO- & C & -CONH-C_5H_4N \\ & \| & \\ & N & -NH-C_6H_4R \end{array}$$

(L_1, $R = p\text{-}CH_3$; L_2, $R = p\text{-}Cl$; L_3, $R = m\text{-}Cl$; L_4, $R = p\text{-}OCH_3$ and L_5, $R = o\text{-}NO_2$).

3-Oxoanilides, such as acetoacetanilides, benzanilides and naphthoylacetanilides, have been the subject of numerous investigations [12–15] but little is known about the acetoacetylaminopyridines or their preparation, or concerning the structural investigation of these compounds and their copper chelates using spectrophotometric methods (UV and visible), proton magnetic resonance (^1H NMR), thermal analysis (TG and DTA) and microanalysis.

The importance of the dyes and their copper complexes under investigations stems from the fact that these complexes can be used as fungicides, have a great influence in the nitrification of soil, can be used in waterproofing, in tanning, in colouring or as parasiticides [16]. α-Arylazoacetoacetanilides have wide industrial applications [17].

EXPERIMENTAL

α-Arylhydrazoneacetoacetylanilides (L_i) were prepared by coupling of the anilide $CH_3COCH_2CONHC_5H_4N$ with diazonium salts. Using a previously described technique, consistently high yields were obtained [18]. The derivatives were crystallized from different solvents to a constant melting point and dried in vacuo. Preliminary studies on these ligands led to the following proposed structures

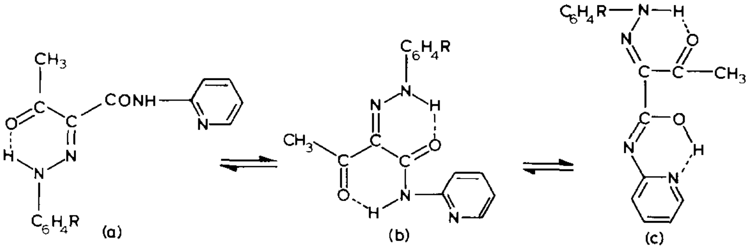

L_i (i = 1–4)

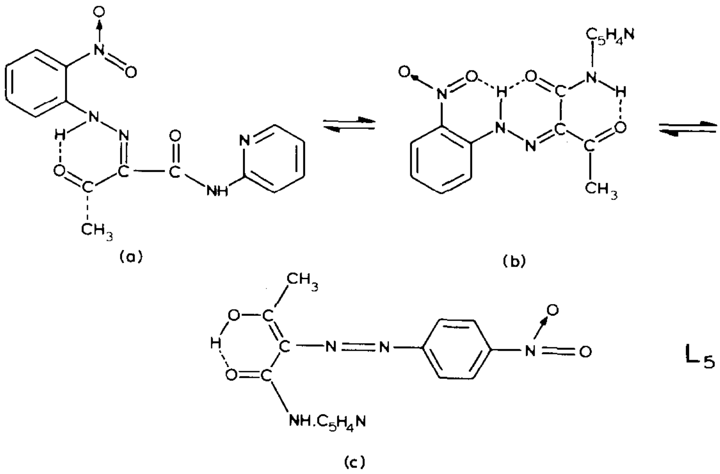

L_5

In order to prepare the copper(II)–L_i complexes (**I_i**, **II**) solutions of these ligands (0.2 g/20 ml 2,4-dioxane) and of copper acetate (0.2 g/20 ml water) were thoroughly mixed, stirred, diluted with water up to 100 ml and left overnight. The following products were formed: green **I_1** (m.p. 139 °C); brownish-green **I_2** (m.p. > 250 °C); brownish-yellow **I_3** (m.p. > 250 °C); yellowish-green **I_4** (m.p. > 250 °C) and a greenish-yellow **II** (m.p. 200 °C). These solid complexes were insoluble in water, slightly soluble in solvents, but soluble in dioxane–water mixture (1 : 1). They were recrystallized from absolute ethanol.

Partial elemental analyses for C, H, N and halogen, and molecular weight (MW) determinations were performed by microanalysts at Cairo University (Table 1).

The absorption spectra of ligands L_i (5×10^{-4} M) and their copper complexes **I_{1-4}** (0.25–0.4×10^{-4} M) and **II** (0.5×10^{-4} M) were measured in dioxane–water mixture (1 : 1), using a PYE Unicam SP 1750 recording spectrophotometer.

Thermal analysis for some ligands ($L_{1,2,5}$) and their complexes (**$I_{1,2}$** and **II**) was also done on a Heraeus Thermal Analyzer, in the Physics Department, University of Cairo.

The IR spectra were recorded as KBr discs on a Beckmann infrared spectrophotometer (INC, Fullation, California, USA) over a wave number range 250–4000 cm^{-1}.

Proton magnetic resonance (^1H NMR) spectra were measured using a Varian EM 360/390 NMR spectrometer (60 MHz) at El-Azhar University.

RESULTS AND DISCUSSION

From the microanalysis data of the separated solid complexes presented in Table 1, the suggested formulae are **I**, $Cu(C_{18}H_{19}N_4O_4)$; **I_2**,

TABLE 1

Elemental analysis of copper(II)–α-arylhydrazoacetoacetylaminopyridine complexes **I** and **II**

Complex [a]		Found (%)				Calculated (%)			
		C	H	N	MW	C	H	N	MW
CuL_1Ac	**I_1**	55.20	4.50	14.20	380.9	55.47	4.88	14.38	389.35
CuL_2Ac	**I_2**	49.4	4.10	14.00	400.5	49.78	3.9	13.66	409.81
$CuL_3 \cdot H_2O \cdot Ac$	**I_3**	47.2	4.4	13.6	423.6	47.68	4.2	13.1	427.85
CuL_4Ac	**I_4**	51.40	4.50	14.10	404.0	50.32	4.68	13.81	403.63
CuL_5	**II_1**	46.10	3.32	14.5	390.0	46.06	3.32	14.33	390.81
$CuL_5 \cdot Ac_2$	**II_2**	51.0	4.8	14.9	440.83	50.68	4.22	15.56	449.83

[a] The suggested formulae of the above complexes from elemental analysis are: **I_1**, $Cu(C_{18}H_{19}O_4N_4)$; **I_2**, $Cu(C_{17}H_{16}O_4N_4Cl)$; **I_3**, $Cu(C_{17}H_{18}O_5N_4Cl)$; **I_4**, $Cu(C_{18}H_{19}O_5N_4)$; **II_1**, $Cu(C_{15}H_{13}O_4N_5)$; and **II_2**, $Cu(C_{19}H_{19}O_8N_5)$.

Cu($C_{17}H_{16}O_4N_4Cl$); $\mathbf{I}_3$, Cu ($C_{17}H_{18}O_5N_4Cl$); $\mathbf{II}_2$, Cu($C_{19}H_{19}O_8N_5$) and the proposed structures are

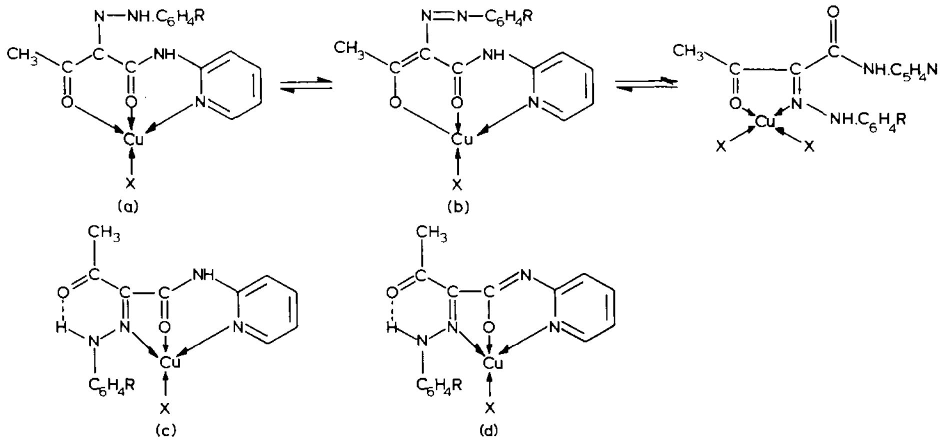

I
(X = H_2O or Ac)

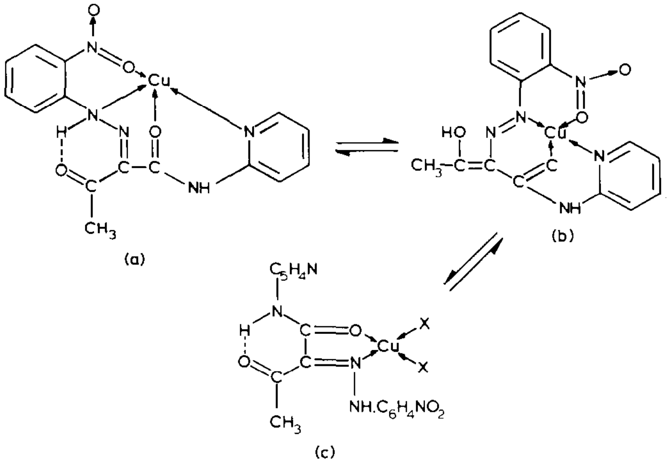

II

The nature of the bonding in these proposed structures can be understood from the following spectra and thermal analyses.

The absorption spectra of ligands L_{1-3} (Fig. 1(a)–(c)) and their possible complexes $\mathbf{I}_{1-3}$ in dioxane (Fig. 1(A)–(C)) show, in the case of the ligands, mainly broad bands at 368–376 nm ($\epsilon = 1.11–3.33 \times 10^4$) which is assigned as $\pi–\pi^\star$ transition of the delocalized π-electrons of the hydrazone group of these ligands. This band shifted to a longer wavelength, 380–388 nm, on formation of $\mathbf{I}_i$ complexes ($\epsilon = 2.9–3.81 \times 10^4$). This red shift and hypthochromic effects may be attributed to the perturbation of the electron system during formation of the $\mathbf{I}_i$ complexes [7]. The absorption spectra of these ligands also show sharp bands at 256–280 nm ($\epsilon = 1.04–8.55 \times 10^4$)

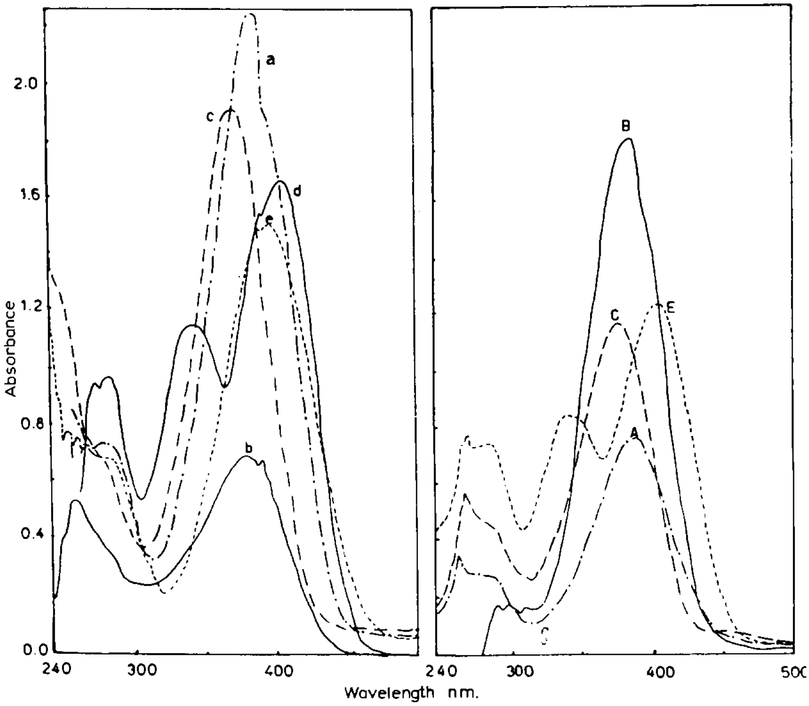

Fig. 1. Absorption spectra of chelating agents L_i (a)–(d) and their copper(II) chelates (A)–(C) and (E).

which may be attributed to the n–$\sigma^\star$ transition within the heterogeneous groups (C=O and C=N). The shift of these bands (260–308 nm), the decrease in their intensities ($\epsilon = 0.1$–2×10^4) and the change of some of them into shoulders, during the formation of the $\mathbf{I}_i$ complexes, may be attributed to a sharing of the C=O and C=N groups in formation of the chelate rings (cf. forms L_i).

The spectrum of the ligand L_5 (Fig. 1(d)) shows three sharp bands at 260, 340 and 408 nm with molar absorptivity 1.41×10^4, 1.88×10^4 and 2.77×10^4, respectively. This may be assigned as n–$\sigma^\star$ transitions in the heterogenous groups (C=O and C=N) together with π–$\pi^\star$ transitions in cyclic rings, which are the results of hydrogen bonding in this ligand (cf. form L_5). The spectrum of complex **II** (Fig. 1(D)) shows sharp broad bands at 400 nm ($\epsilon = 1.2 \times 10^4$) and at 340 nm ($\epsilon = 8.4 \times 10^3$) which are attributed to π–$\pi^\star$ transitions in the π-electron system of complex **II**. The first is related to the hydrazone group of the tetradentate ligand L_5. The spectrum of complex **II** also shows a shoulder starting at 272 nm ($\epsilon = 7.4 \times 10^3$) and a small sharp band at 260 nm ($\epsilon = 7.8 \times 10^3$). These bands may be attributed to n–$\sigma^\star$ and/or π–$\pi^\star$ transitions in the heterocyclic chelate rings of complex **II**. The slight blue shift of the bands of ligand L_5 and the decrease in their intensity

TABLE 2

Assignment of the fundamental group vibrations of copper(II)–α-arylhydrazoacetoacetylaminopyridine (L_{1-5}) complexes (**I**$_{1-5}$ and **II**$_{1,2}$)

Compound	Mode									
	ν(OH)	ν(NH)	ν(CO)	ν(NO_2)	ν(C=N)	ν(N=N)	ν(CONH)	ν(C–O)	ν($COCH_3$)	ν 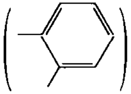	ν 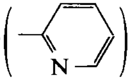
L_{1-4}	3350– 3500 b	2900– 3200 b	1740– 1760 w,b	–	1550 s,sh	1590 sh	1650 s	1260– 1300 sh	1350 s,sh 1420 s,sh	1470 s,sh 1500 s,sh 1150– 1200 s,sh	3020 w,sh 3040 s,sh 700 s,sh
I$_{1-5}$	3400 sh,b	2900– 2980 sh,w	1710 1740 1780 w,sh	–	1560 w	1580 w 1620 w	1650 w	1280– 1300 w,sh	1360 w,sh 1450 w,sh	1490 w,sh 1500 w,sh	3000 vs 3030 w,sh 700 vs
L_5	3310– 3500 w,b	3020– 3120 s,b	–	1310 s,sh 1280– 1300 s,sh,b 1550 s,sh	1520 w,b	1590 s,sh	1660 vs,sh	–	1340 s,sh 1400 s,sh	1470– 1490 sh,b 1130,1160 1190 s,sh	3020– 3050 b 3070 w
II$_{1,2}$	3300– 3500 vsh,b	2900–2980 w,b	–	– 1540 w,b	1510 w,b	1610 s,sh	1660 w,sh	–	1330 w,sh	1470–1490 sh,b 1130,1170 1190 s,sh	

vsh = very sharp, s,sh = strong sharp, w = weak, vw = very weak, sh,b = sharp broad, b = broad.

is mainly attributed to stabilization of the electron system of this ligand during formation of complex **II**.

To understand the nature of the bonding in these ligands and their complexes, assignment of IR bands [19] is necessary (Table 2). In the spectra of the ligands L_{1-4}, the broad band at 3350–3500 cm^{-1} is assigned as $\nu(OH)$ of the possible enol form and/or hydrogen bonded carbonyl groups of these ligands (cf. form L_i). On formation of complexes $\mathbf{I}_{1-3}$ (cf. form **I**), this band becomes a sharp broad one centred at 3400 cm^{-1} (lower energy) indicating bonding between L_i and the external ligand molecules (H_2O and/or acetate groups) to the central copper(II) ions via oxygen-containing groups eg. CO and CONH, by ionic and coordinate bonds (**I**(a)–(d)). The sharing of these groups in bond formation of complex **I** is confirmed by the shift of the weak broad band at 1740–1760 cm^{-1}, assigned as $\nu(CO)$, into three weak sharp bands at 1710, 1740 and 1760 cm^{-1}; by the shift of the strong sharp bands at 1350 and 1470 cm^{-1}, assigned as $\nu(COCH_3)$, into weak sharp bands at 1360 and 1430 cm^{-1} and, finally, by the decrease in intensity of the strong sharp band at 1650 cm^{-1}, assigned as $\nu(CONH)$. The sharing of nitrogen-containing groups in complex formation is also indicated by the shift of the sharp bands of L_i at 1950 cm^{-1} of $\nu(N{=}N)$, at 1550 cm^{-1} of $\nu(C{=}N)$, and of the broad band at 2900–3200 cm^{-1}, of $\nu(NH)$, into weak bands at 1580, 1560 and 2900–2980 cm^{-1}, respectively. This shift to lower energies and the weakness of their intensities indicates a stabilization of the electron system of the ligands L_i by chelation of these groups to Cu(II) ions via formation of $M \cdots N$ bonds in heterogenous six-membered chelate rings (cf. form **I**).

In the case of the *o*-NO_2 derivative L_5, the weak broad band at 3331–3500 cm^{-1}, which was assigned as $\nu(OH)$ of its hydrogen bonded form, of enol or of any possible hydrogen bonded carbonyl groups, was changed into a very sharp broad band at 3300–3500 cm^{-1} as a result of the coordination of this ligand or other external ligands (e.g. H_2O or acetate) to Cu(II) ions via oxygen-containing centres. The changes, of the sharp broad band at 3020–3120 cm^{-1}, assigned as $\nu(NH)$, into a weak broad band at 2900–2980 cm^{-1}; the shift of the weak broad band at 1520 cm^{-1} of $\nu(C{=}N)$ to 1510 cm^{-1}; the change in the strong sharp band at 1590 cm^{-1}, assigned as $\nu(C{=}N)$, into a weak band at 1610 cm^{-1} and finally, the change in the strong sharp bands at 1340 and 1440 cm^{-1}, assigned as $\nu(COCH_3)$, into a weak sharp band at 1330 cm^{-1}, are all attributed to a lowering of the energy of the electron system of the ligand L_5 as a result of its chelation to Cu(II) ions via these groups containing heterogenous atoms, by the formation of $M \cdots O$ and $M \cdots N$ bonds. The strong sharp bands at 1310 and 1550 and the sharp broad band at 1280–1300 cm^{-1}, assigned as $\nu(NO_2)$ vibrations, completely disappeared in formation of complex **II**, which indicates the sharing of the *o*-NO_2 group in the formation of this complex (cf. form **II**).

Generally, in all ligands, the broad band at 3020–3050 cm^{-1} and the weak band at 3670 cm^{-1}, assigned as pyridine ring vibrations, either completely disappear or are shifted to lower frequencies in the IR spectra of the complexes; this suggests a possible sharing of the ring system in chelation via the nitrogen atom of the pyridine ring, which stabilized the electron system of the pyridine ring.

The proton magnetic resonance spectra of L_i show signals at 2.4 and 2.8, attributed to the three protons of *p*-methyl (of L_1) and of CH_3CO (of L_{1-3}), respectively; this was confirmed by the integration curves which corresponds to six protons, three in each group [19]. The signals corresponding to protons of pyridine phenyl rings appear in the range 7.2–9.6 ppm, confirmed by the integration curve representing seven protons. The 8th proton which appears separately at 10 ppm is that of C–H at the 3-position of the aminopyridine part of L_i. The signal at 9.8–12 ppm refers to protons of hydrazone and amide groups, because it completely disappears in deuterated water.

The ^1H NMR spectra of $\mathbf{I}_i$ and **II** complexes indicate the complete change in multiplicity of the ligand signals at 7.6–9.6 and at 9.8–12 ppm and their shift lower energies at 7.4–11.6 ppm. These changes and shifts are attributed to the sharing of the pyridine ring system, and of the amide and hydrazone groups in the formation of these complexes.

Thermal analysis: DTA and TG

In this laboratory, thermal analysis techniques are widely applied in studying the structure of various substances e.g. redox products [20,21] and complexes [7,22], especially those of copper(II) with ligands containing nitrogen and oxygen as centres of chelation. Very interesting structural changes occur during thermal treatment of copper complexes; this suggested that we study more chelates in this work (Table 3).

In the present investigation, some ligands ($L_{1-3,5}$) and some complexes ($\mathbf{I}_{1,2}$ and **II**) were subjected to thermal analysis (DTA and TG) as shown in Figs. 2 and 3, in order to elucidate the proposed structures of these ligands and their complexes. DTA curves for the ligands are shown in Fig. 2(a)–(d) whereas those for the complexes are shown in Fig. 2(A)–(D). Curves (a)–(c) show a very sharp endotherm at 125 °C (a), a broad endotherm in the temperature range 150–155 °C (b) and a sharp one at 130 °C (c), followed by a very large endothermic shift from the base line beginning at 170 °C (a), 185 °C (b) and at 160 °C (c), and finally a small exotherm at 270 °C in the case of (a) only. The first endotherms of these ligands may be attributed to the decomposition of hydrogen bonding in the general structural form L_i. The shift in the base line is essentially due to the change in heat capacity following the above decomposition, as a result of the increase in entropy of these systems. In the case of ligand L_1 (Fig. 2(a)), the small exotherm at 270 °C may be attributed to some internal chemical changes in the structure of this ligand without chemical decomposition. In the case of ligand L_5 (Fig.

TABLE 3

Mass loss of arylhydrazone acetoacetylaminopyridine (L_i) complexes ($\mathbf{I}_1$, $\mathbf{I}_3$ and **II**) with copper (II)

Complex	Temp. range (°C)	Decomposition products lost	Wt. loss (%)	
			Estm.	Calcd.
$\mathbf{I}_1$	96–186	$CH_3{\cdot}COO$	16.0	15.50
	194–270	CO_2	12.0	11.60
$\mathbf{I}_3$	68–100	H_2O of hydration	4.0	4.26
	106–130	coord. H_2O	4.0	4.26
	130–158	CH_3COO	14.0	13.95
	168–250	$\frac{1}{2}Cl_2$	8.0	8.30
II	106–250	$2CH_3COO$	26.0	26.76
	or			
	106–150	CH_3–CH_3	6.0	6.76
	150–250	$2CO_2$	20.0	20.00

2(d)), there is a sharp endotherm at 195 °C and another broad one centred at 218 °C. The first may be attributed to the dissociation of hydrogen bonds in the L_5 forms but the latter may be related to dissociation of the strong hydrogen bond of the NO_2 group in the *o*-position of the phenylhydrazone skeleton (cf. form L_{5b}).

Generally, it is noticeable that the decomposition temperature of hydrogen bonds in these ligands is related to the strength of these bonds as a result of the electron withdrawing ability of the substituent in the phenyl hydrazone derivatives e.g. *p*-Me at 125 °C, *p*-Cl at 185 °C, *o*-NO_2 at 195 °C and 218 °C, and *m*-Cl at 130 °C. This means that the electron-withdrawing groups in the *o*- or *p*-position of the phenylhydrazone ring increase the strength of the hydrogen bonds, while electron-repelling groups, such as the *p*-methyl group, decrease the possibility of formation of these bonds; the *m*-substituent e.g. *m*-Cl has an intermediate effect.

Fig. 2(a) shows the DTA curve of complex $\mathbf{I}_1$ of the *p*-methyl derivative. This curve shows endotherms at 50–100 °C and several small exotherms at 125–150 °C, 180–200 °C, 225–237 °C, 262–275 °C and 300–325 °C which are attributed to several non-vigorous chemical reactions and to the crystallization or ordering of this metastable complex. These chemical reactions which occur with temperature changes can only be explained by the change of the square planar complex (green colour) into the tetrahedral or distorted octahedral form (brown) by formation of additive bonds or by the strengthening of the original bonds between copper ions and the chelation centres of L_1. The exotherms at 180–275 °C may also be attributed to decomposition of the lost acetate group into CO_2 and $CH_3^{\cdot}$ active free radicals, as confirmed by TG (Fig. 3(a)).

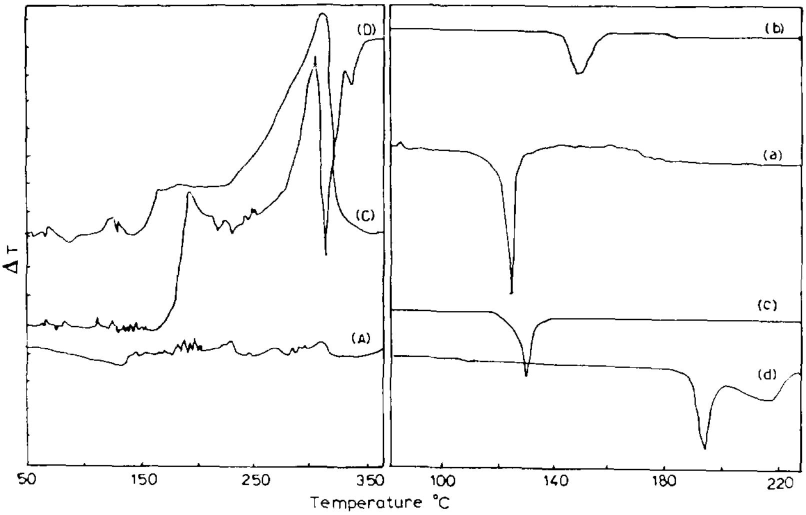

Fig. 2. DTA curve for ligands L_i (a)–(d) and their chelates (A), (C) and (D).

Fig. 2(C) shows the DTA curve for the I_3 complex. There are two endotherms at 68–100 and 130–155 °C which may be due to the loss of H_2O and acetate ligands, respectively. It shows small exotherms at 80 and 125 °C which may refer to extra bonds formed in this complex, with heating and/or increasing of bond strength during its change from one form to another. It also shows an exothermic base line shift starting at 173° C which denotes a change in heat capacity of the system due to its stabilization by heating at this temperature. The abrupt broad exotherm occuring at 312–322 °C refers to internal changes in the chemical bonds between L_3 and Cu(II) ions as a

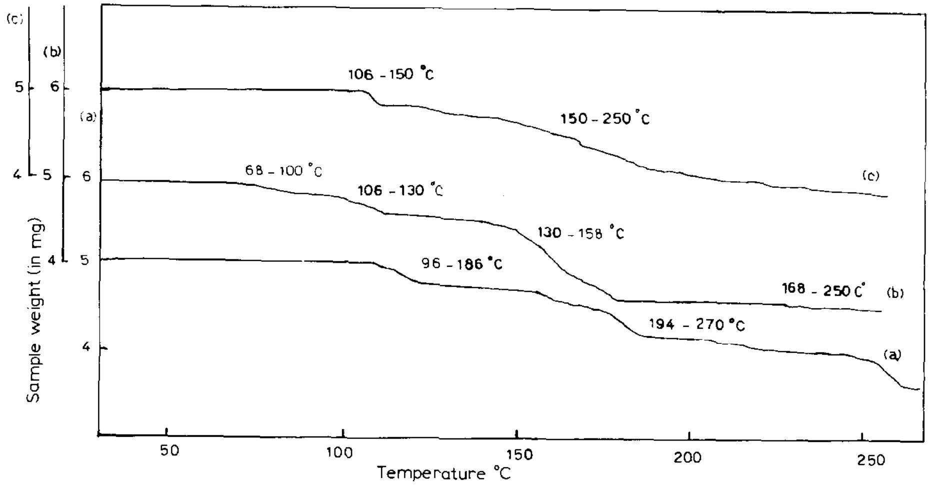

Fig. 3. TG curve for arylhydrazoneacetocetylaminopyridine–copper(II) chelates.

consequence of rearrangement of the shape of this complex with temperature increase. It may also relate to the possible decomposition of the lost acetate group into $CH_3^{\bullet}$ free radical and CO_2 gas and $Cl^{\bullet}$ into $\frac{1}{2}Cl_2$ gas.

The DTA curve of complex **II** of *o*-NO_2 derivative (L_5) with copper ions are represented in Fig. 2(D). It shows a broad endotherm at 130–160 °C and a very broad exotherm at 180–225 °C, a sharp exotherm at 312 °C, then immediately a very sharp endotherm at 320 °C and a sharp exotherm at 330 °C and finally, an immediate sharp endotherm at 338 °C. The endotherm at 130–160 °C may be attributed to the loss of two acetate groups as indicated by TG. The first broad sharp exotherms may be attributed to the enhanced stability of this complex by formation of extra bonds and chelate rings in the temperature range 180–312 °C or it may be attributed to the decomposition of the lost acetate groups. The formation of such extra bonds may be followed by decomposition of other bonds of the ligand during heating (e.g. hydrogen bonds), confirmed by the appearance of a sharp endotherm at 320 °C. This may also be explained by the fragmentation of part of the ligand in the complex formation (cf. form **II**(b)). This fragmentation process is followed by a rearrangement of the remaining part of the complex, as indicated by the appearance of sharp exotherm at 330 °C. This is followed by fusion of the remaining part of the complex and volatilization of the decomposed part, as indicated by the final endotherm at 338 °C.

Fig. 2 illustrates TG curves for complexes $\mathbf{I}_{1,2}$ and $\mathbf{II}_1$, respectively, within a temperature ranging from room temperature up to 480 °C. The estimated mass losses were computed based on the TG results and the calculated mass losses were computed using the results of microanalysis (Tables 1 and 3).

For the TG of complex $\mathbf{I}_1$ (Fig. 3(a)), the estimated mass loss is 16.0% which reasonably accounts for the loss of the acetate group (calculated mass loss 15.5%) which occurs at 96–186 °C and its decomposition into CO_2 and free radicals $CH_3^{\bullet}$ occurring at 194–290 °C. The loss of the acetate group also correlates with the appearance of endotherms in the temperature range 50–100 °C in the DTA curves of this complex. The last decomposition explains the appearance of exotherms at 180–275 °C in the DTA curve (cf. Fig. 2(A)).

The TG curve of the complex $\mathbf{I}_3$ (Fig. 3(b)) gives the first estimated mass loss of 4.0% within the temperature range 68–100 °C which may be due to the liberation of water of hydration (calculated mass loss 4.26%). This is immediately followed by another mass loss of 4.0% at 106–130 °C which is due to the loss of coordinated water (calculated mass loss 4.26%). This explains the endothermic shift of the DTA base-line at 68–130 °C. The loss of acetate ligand molecule (estimated mass loss 14.0%) occurs at 168 °C (calculated mass loss 13.95%). This is followed by an abrupt mass loss of 8.0% at 168–250 °C due to the loss of $Cl^{\bullet}$ free radicals which react to give Cl_2 gas (calculated mass loss 8.3%), which explains the appearance of an abrupt broad exotherm at 260 °–300 °C followed by the pronounced endothermic base-line shift in the DTA curve after this temperature range.

On the other hand, the TG curve of product **II** (Fig. 3(c)) exhibits a single estimated mass loss of 26% within the temperature range 106–250 ° C which might be attributed to the loss of two acetate ligand molecules from the moiety of this complex (calculated weight loss 26.26%). This may be subdivided into two mass losses. The first occurs at 106–150 ° C (estimated mass loss 6%) due to the decomposition of two acetate groups into $CH_3^{\cdot}$ free radicals that react to form CH_3–CH_3 gas (calculated mass loss 6.76%). The second mass loss at 150–120 ° C (estimated 20%) is due to the decomposition of two carboxylic groups of the lost acetate groups to form two CO_2 gas molecules (calculated mass loss 20%). These losses explain the appearance of a broad endothermic shift of the DTA base-line at 130–160 ° C followed by a very broad exotherm at 180–225 ° C.

ACKNOWLEDGEMENT

Thanks are due to Dr. R.S. Farag, Associate Prof. of Organic Chemistry, Faculty of Science, El-Azhar University, for his interest and for doing all the NMR measurements.

REFERENCES

1 G.A. Barclay and C.H.L. Kennard, J. Chem. Soc, (1951) 5244; F. Hanic, D. Stempelova and K. Hanicova, Acta Crystallogr., 17 (1964) 633; J.K. Kochi and R.V. Subramian, Inorg. Chem., 4 (1961) 1527.
2 G.A. Barclay and C.H.L. Kennard, J. Chem. Soc., (1961) 524; E. Kokat and R.L. Martin, Inorg. Chem., 3 (1964) 1306.
3 H.J. Harries, S. Savage, G. Wright and N. Logan, J. Inorg. Nucl. Chem., 31 (1969) 2477.
4 G. Stoeckelmann, A. Kettrup and H. Specker, Z. Anorg. Allg. Chem., 372 (1970) 134.
5 A. Syamal, J. Indian Chem. Soc., 45 (1968) 374.
6 L. Wolf and K. Wetzel, Chem. Ber., 90 (1957) 1007.
7 M.A. Zayed and F.A. Nour El-Dien, Thermochim. Acta, 114 (1987) 359.
8 W.E. Hatfield, H.D. Dedon and S.M. Horner, Inorg. Chem., 4 (1965) 1181.
9 A.E. Martell and M. Calvin, Chemistry of the Metal Chelate Compounds, Prentice Hall, New York, 1952.
10 J.C. Bailar, Jr., (Ed.), Chemistry of Coordination Compounds, Rheinhold, New York, 1956.
11 R.D. Gillard and G. Wilkinson, J. Chem. Soc., (1963) 5399.
12 S.M. Parmerter, Org. React., 10 (1959) 1.
13 M.I. Ali, M.M.S. Al-Morsy, H.A. Hammuda and M.A.F. Sharaf, Egypt. J. Chem., 22 (1979) 179.
14 M.I. Ali, M.M.S. El-Morsy, N.M. Hassan and M.A.F. Sharaf, Z. Naturforsch., 33 (1978) 425.
15 H.M. Fahmy, M.M.S. El-Morsy and M.A.F. Sharaf, J. Electroanal. Chem., 94 (1978) 165.
16 Compagnie Francais de Matières Colorantes, Fr. 1 (1957) 130, 229.

17 A. Arcoria, S. Fisichella and M. Torre, Chim. Ind. (Milan), 53(6) (1971) 565.
18 A.A. El-Damaty, Reactions with some active methylene compounds, Ph.D. Thesis, Faculty of Science, University of Cairo, 1986.
19 B.S. Furniss, A.J. Hannaford, V. Rogers, P.W.G. Smith and A.R. Tatchell, Vogel's Textbook of Practical Organic Chemistry, ELBS and Longman, London, 4th edn., 1980, p. 954.
20 M.A. Zayed, Thermochim. Acta, 111 (1987) 103.
21 M.A. Zayed and F.A. Nour El-Dien, Thermochim. Acta, 113 (1987) 117.
22 M.A. Zayed, M.M. Khater, M.S. Rizk, and H.M. Abd El-Fattah, Thermochim. Acta, 73 (1984) 217.